

## Hydrodynamics of Nanoscopic Capillary Waves

R. Delgado-Buscalioni,<sup>1,\*</sup> E. Chacon,<sup>2</sup> and P. Tarazona<sup>1</sup>

<sup>1</sup>*Depto. Física Teórica de la Materia Condensada, Universidad Autónoma de Madrid, Campus de Cantoblanco, Madrid, E-28049, Spain*

<sup>2</sup>*Instituto de Ciencia de Materiales de Madrid Consejo Superior de Investigaciones Científicas Cantoblanco, Madrid E-28049, Spain*  
(Received 13 June 2008; published 5 September 2008)

The dynamics of nanoscopic capillary waves on simple liquid surfaces is analyzed using molecular dynamics simulations. Each Fourier mode of the surface is obtained from the molecular positions, and its time behavior compared with the hydrodynamic prediction. We trace the transition from propagating to overdamped modes, at short wavelengths. The damping rate is in very good agreement with the hydrodynamic theory up to surprisingly small wavelengths, of about four molecular diameters, but only if the wave number dependent surface tension is considered. At shorter scales, surface tension hydrodynamics break down and we find a transition to a molecular diffusion regime.

DOI: [10.1103/PhysRevLett.101.106102](https://doi.org/10.1103/PhysRevLett.101.106102)

PACS numbers: 68.03.Kn, 68.03.Cd, 68.03.Hj

Ripples at a fluid surface are dominated by gravity at wavelengths at the scale of meters, while for wavelengths  $\lambda \lesssim 1$  cm they become capillary waves (CW) dominated by the surface tension. The hydrodynamic theory [1–3] for CW predicts another crossover from the usual propagative mode to an overdamped nonpropagative mode set by the balance between the surface tension and viscous forces. Such crossover has been experimentally observed at  $\lambda \sim 0.1$  mm, in gel and polymer systems [4], complex, very viscous fluids [5], and ionic liquids [6]. In simple fluids, the overdamped hydrodynamic regime is predicted for much smaller wavelengths,  $\lambda \sim 10\sigma$  in terms of the molecular diameter  $\sigma$ . A fundamental question which remains open is the validity of the hydrodynamic description at such a nanometric scale, very close to the molecular discreteness of the fluid.

The problem is closely related to the experimental and theoretical [7,8] analysis of the thermally excited CW fluctuations in liquid surfaces, usually described in terms of  $\gamma(q)$ , the effective surface tension for CW with wave vector  $q = 2\pi/\lambda$ . The deviation of this function from its thermodynamic limit  $\gamma(0) = \gamma_0$  is a subject of controversy, with claims of an enhanced CW regime at nanometric scale [7,9] characterized by  $\gamma(q) < \gamma_0$ . The experimental evidence [10] and the theoretical basis for that phenomena [8] have been recently criticized, but still the problem of how to measure or calculate  $\gamma(q)$  is a crucial question for the analysis of x-ray diffraction experiments on liquid surfaces.

Molecular dynamics (MD) simulations allow the study of these fundamental questions, connecting the molecular structure of the fluid surface and its description as an intrinsic surface (IS),  $z = \sum_{\mathbf{q}} \hat{\xi}_{\mathbf{q}} \exp(i\mathbf{q} \cdot \mathbf{R})$ , that describes the instantaneous shape of the fluctuating interface, with thermal average parallel to the  $\mathbf{R} = (x, y)$  plane. The Capillary Wave Theory (CWT) [11] assumes that the IS Fourier components  $\hat{\xi}_{\mathbf{q}}$  may (somehow) be obtained from

the molecular positions, and it opens a direct structural route to measure the wave vector dependent surface tension from the mean square amplitude of the CW thermal fluctuations over a transverse area  $A$  [12,13],

$$\gamma_s(q) = \frac{k_B T}{q^2 \langle |\hat{\xi}_{\mathbf{q}}|^2 \rangle A}. \quad (1)$$

This structural method gives the correct macroscopic limit  $\gamma_s(0) = \gamma_0$ , but for  $q\sigma \gtrsim 0.5$ , there is a strong dependence of  $\gamma_s(q)$  on the specific proposals to get  $\hat{\xi}_{\mathbf{q}}$  from the molecular positions [12]. The simplest choice, based on a local Gibbs dividing surface, gives an unphysical  $\gamma_s(q) \sim 1/q^2$  decay [14]. Recent developments have produced and tested a specific proposal [13], known as the Intrinsic Sampling Method (ISM), to obtain  $\hat{\xi}_{\mathbf{q}}$  from a self consistently defined surface layer, based upon the set of molecules ascribed to the liquid boundary. The ISM main parameter is the surface layer density  $n_s$ , which has to be optimized to get the sharpest molecular structure near the interface. Still,  $n_s$  and thus  $\gamma_s(q)$  may have significant error bars due to the inherent uncertainty of what is the outmost molecular layer in a disordered fluid surface. Therefore, the use of the ISM has been restricted to relatively stiff liquid surfaces, with  $\gamma_0 \sigma^2 / (k_B T) \gtrsim 0.4$ , or  $T/T_c \lesssim 0.85$  for simple fluids ( $T_c$  is the critical temperature).

In this Letter, we compare structural and dynamical analyses to find out that hydrodynamics provides a much more robust physical route to the surface tension wave vector dependence,  $\gamma_d(q)$ . Moreover, the optimal occupation density predicted from the ISM analysis precisely provides  $\gamma_s(q) = \gamma_d(q)$ , hence physically consistent structure and hydrodynamics. By comparing MD results with the hydrodynamic prediction based on the optimal  $\gamma_s(q)$ , we prove that CW hydrodynamics remain valid up to surprisingly large wave numbers,  $q\sigma \lesssim 2$ , well above the validity of the macroscopic surface tension prediction

( $q\sigma \lesssim 0.5$ ). At even smaller scales ( $q\sigma \gtrsim 2$ ), molecular diffusion becomes the slowest mode and surface tension hydrodynamics gradually break down.

Hydrodynamic analysis, either based on the linearized Navier-Stokes equations [1,2] or on linear response theory [3], gives the dispersion relation for surface modes,

$$D(q, \tilde{\omega}) = \frac{\gamma q^3}{\rho} - (\tilde{\omega} + 2i\nu q^2)^2 - 2\nu^2 q^4 \left[ 1 - \frac{i\tilde{\omega}}{\nu q^2} \right]^{1/2}, \quad (2)$$

where  $\rho$  is the liquid density while  $\nu = \eta/\rho$  and  $\eta$  are the kinematic and dynamic shear viscosities. The mode complex frequency  $\tilde{\omega}(q) = \omega(q) + i\Gamma(q)$ , which determines the temporal behavior of the surface  $\hat{\xi}_q(t)$ , is given by the solutions of  $D(q, \tilde{\omega}) = 0$ . Above a certain wave number,  $q > q_{cr} \sim \gamma\rho/\eta^2$ , the dispersion relation (2) predicts a transition from the usual propagative capillary modes to overdamped waves. The damping rate by viscous forces  $\nu q^2$  overpowers the restoring frequency of surface tension  $(\gamma q^3/\rho)^{1/2}$ , and the real part of the complex frequency vanishes  $\omega = 0$ . Surface fluctuations then become exponentially damped at a rate given by  $\Gamma = i\tilde{\omega}$ , which goes roughly like  $\Gamma \sim q\gamma/\eta$  [3]. In simple liquids, this crossover takes place at  $q_{cr}\sigma \sim 0.3$ ; therefore, the analysis of the overdamped regime, at larger  $q$ , requires to take into account the dependence of the transport coefficients on the wave number. While  $\gamma_s(q)$  may be provided by Eq. (1), the generalized shear viscosity  $\eta(q)$  of the LJ liquid, has been evaluated in several works, either using the generalized hydrodynamics theoretical framework [15,16] or from nonequilibrium MD simulations [17,18].

In order to observe the propagative-overdamped transition in MD simulations of simple liquids, we start with the soft-alkali (SA) cold-liquid model [19]. At a temperature  $kT = 0.212\epsilon$ , the SA liquid has a very stiff surface and a reasonably high  $q_{cr} = 0.8/\sigma$ , which permits us to observe the transition using simulation boxes of transverse size  $L \approx 20\sigma$  (i.e.,  $q \geq 2\pi/L \approx 0.3/\sigma$ ). MD simulations were done within periodic boundary conditions, in two different simulation boxes with linear transverse size  $L = 9.025\sigma$  and  $L = 18.05\sigma$ . We prepare the system with a liquid slab of thickness  $\delta \approx 3L$  (thick enough to avoid the hydrodynamic coupling across the liquid bulk) and set much larger periodic conditions on the  $z$  direction ( $L_z = 90\sigma$  and  $120\sigma$ , respectively) to get two independent liquid surfaces, separated by a rarefied vapor phase. Simulations were done in the microcanonical ensemble, although similar results were obtained in the  $NVT$  ensemble, provided a thermostat with large enough inertial time. The time step was  $\delta t = 0.005\tau$  [with  $\tau \equiv \sigma(\epsilon/m)^{1/2}$  the usual LJ time unit] and configurations were sampled each  $\Delta t_{\text{samp}} = 0.05\tau$  or  $0.5\tau$  (depending on the CW time scale). Configurations were analyzed using the method given in Ref. [13], to obtain the instantaneous intrinsic surface Fourier components  $\hat{\xi}_q(t)$  for each allowed wave vector

$[\mathbf{q} = 2\pi(\nu_x, \nu_y)/L]$ , with integer  $\nu_x, \nu_y$ . Figure 1 shows the angular frequency  $\omega_d$  and the damping rate  $\Gamma_d$  extracted from MD, by fitting the surface modes auto-correlation function (ACF)  $\langle \hat{\xi}_q(t) \hat{\xi}_q^*(0) \rangle$  to  $\langle |\hat{\xi}_q|^2 \rangle \times \exp(-\Gamma_d t) \cos(\omega_d t)$  (see insets). The corresponding hydrodynamic predictions  $\Gamma_o$  and  $\omega_o$ , obtained by inserting the macroscopic surface tension  $\gamma_0$  and viscosity  $\eta_0$  in the dispersion relation (2), are indicated with dashed lines in Fig. 1, while the use of our best ISM estimate for  $\gamma_s(q)$  into Eq. (2) leads to  $\Gamma_s$  and  $\omega_s$ , shown in solid lines. Both theoretical predictions correctly forecast the loci of the oscillatory branch and the transition to the overdamped regime obtained in MD simulations. This excellent agreement confirms the validity of Eq. (2) in the present context. Notice that the transport properties of the SA liquid show little dependence on the wave number:  $\gamma_s(q) \approx \gamma_0$  up to  $q\sigma \lesssim 1.0$  while the shear viscosity  $\eta(q) \approx \eta_0$  for  $q\sigma \lesssim 1.5$ . We will now focus on “more typical” liquids to analyze the surface behavior at larger  $q$ , within the strong damping regime.

Typical liquids have much higher triple point temperature than the SA model. Therefore, they have to be studied at higher temperatures, lower surface tension, and hence, smaller crossover wave number. The results obtained for the Lennard-Jones (LJ) liquid presented in Fig. 2 correspond to  $q_{cr}\sigma = 0.32$ , so the entire range of  $q$  allowed in our simulation box (size  $L = 10.46\sigma$ ), is now within the overdamped regime. In this case, the damping rate  $\Gamma_d$ , directly extracted from the exponential decay of the ACF, starts to deviate from the macroscopic hydrodynamic prediction  $\Gamma_o$  above  $q\sigma \gtrsim 0.5$  and, around  $q\sigma \approx 2$ ,  $\Gamma_d$  is 5

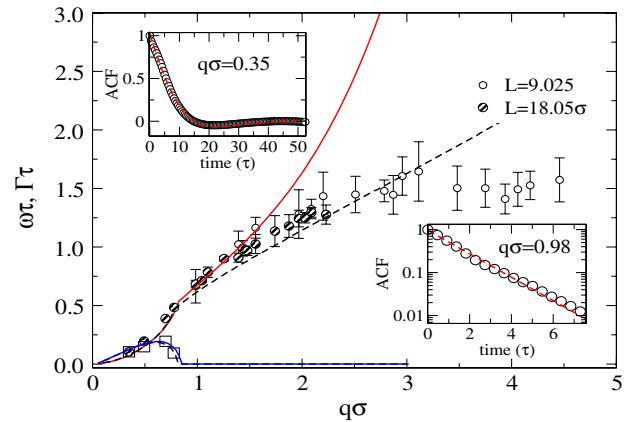


FIG. 1 (color online). The decay rate  $\Gamma$  and angular frequency  $\omega$  wave number dependence of capillary modes in a soft alkali (SA) liquid model at  $T = 0.212\epsilon/k$ , density  $\rho = 1.17\sigma^{-3}$ , surface tension  $\gamma_0\sigma^2/(kT) \approx 8.23$ , and shear viscosity  $\eta = 1.5\epsilon\tau/\sigma^3$ . Symbols correspond to  $\Gamma_d$  (circles) and  $\omega_d$  (squares) obtained from MD simulations of different box transversal sizes  $L$ . Lines are the hydrodynamic predictions, using  $\gamma_s(q)$  (solid line) and  $\gamma_0$  (dashed line). Standard Lennard-Jones units are used throughout, here  $\tau = \sigma(\epsilon/m)^{1/2}$ . Insets show normalized ACF and fitting functions.

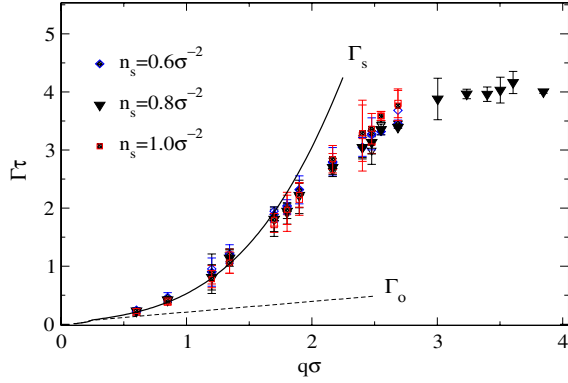


FIG. 2 (color online). The decay rate  $\Gamma$  of CW's in a Lennard-Jones liquid at  $T = 0.848\epsilon/k$ , density  $\rho = 0.738\sigma^{-3}$ , viscosity  $\eta_0 = 1.5\epsilon\tau/\sigma^3$  [23], and surface tension  $\gamma_0\sigma^2/(kT) = 0.653$ . Symbols are obtained from MD simulations by fitting the ACF  $\langle \hat{\xi}_q(t)\hat{\xi}_q^*(0) \rangle$  to  $\langle |\hat{\xi}_q|^2 \rangle \exp(-\Gamma_d t)$ . Values of the first layer occupation parameter  $n_s$  are indicated. Solid line is the hydrodynamic prediction using the optimal  $\gamma_s(q)$  [which corresponds to  $n_s = (0.70 \pm 0.05)\sigma^{-2}$ ] and dashed line to the macroscopic limit, using  $\gamma_0$ . Simulations were done within a box with transverse size  $L = 10.46\sigma$  and liquid slab of width  $\delta = 30\sigma$  (filled symbols) and  $\delta = 70\sigma$  (open symbols).

times larger than  $\Gamma_0$ . In the LJ case,  $\Gamma_0$  severely underestimates the damping rate obtained from MD simulations at all the temperatures considered (e.g., by a factor 6 at  $kT = 0.933\epsilon$  and  $q\sigma \approx 2$ ).

The clue to understand this discrepancy comes from the values of  $\gamma_s(q)$  extracted from (1). As shown in Fig. 2, the damping rate  $\Gamma_s$  obtained from the optimal ISM choice extends the agreement with the exponential decay of the ACF up to  $q\sigma \approx 2$ . It is most remarkable that the continuous hydrodynamic description of the surface fluctuations may be valid down to wavelength of about three molecular diameters, with the use of an independently obtained function  $\gamma_s(q)$ . Such agreement is kept at other temperatures in the LJ fluid, and also in the cold-liquid SA model (up to  $q\sigma \approx 1.5$ , see Fig. 1). These results are a strong evidence for the validity of the hydrodynamic description of CW fluctuations at the nanoscale [1–3], and they also validate the ISM used to get the IS shape from the atomic positions. To confirm these claims, we still have to analyze the dependence of  $\Gamma_d$  on the detailed procedure to get  $\hat{\xi}_q$  from the molecular positions.

The ISM [12,13] has proven to be very useful in extracting the intrinsic density profiles of the fluid interfaces [20] out of the CW blurred averages. The results for atomic, molecular and metallic fluids have shown that the optimal  $n_s$ , providing the sharpest view of the molecular layering, can be satisfactorily determined, and that it contains a physically relevant information on the interfacial structure. However, particularly near the critical point, it still presents relatively large error bars, thus making the determination of  $\gamma_s(q)$  a much delicate matter. In the case of the

LJ liquid at  $kT = 0.736\epsilon$ , the optimal choice [13] is to take  $n_s = 0.75 \pm 0.05$  atoms per  $\sigma^2$  area. The dashed lines in Fig. 3 show the resulting  $\gamma_s(q)$  if we exaggerate that uncertainty taking surface layer densities between  $n_s = 0.6/\sigma^2$  and  $n_s = 1.0/\sigma^2$ . Notice that, for the same atomic configuration, the choice of the  $n_s$  parameter leads to a different IS shape. Clearly, if the surface dynamics were also to depend on the choice of  $n_s$ , then it will not be possible to infer the existence of the proper definition of the intrinsic surface.

Fortunately, as illustrated in Fig. 2, we observe that the value of  $\Gamma_d$  extracted from the time ACF of the surface modes is very insensitive to the value of  $n_s$ . A definite proof requires a dynamical measure of the  $q$ -dependent surface tension  $\gamma_d(q)$ . The result of such evaluation, done via the numerical inversion of the hydrodynamic relation for the damping rate  $\Gamma = i\tilde{\omega}(q; \gamma, \eta)$  arising from  $D(q, \tilde{\omega}) = 0$  in Eq. (2), is shown in Fig. 3. It enables us to draw two interesting conclusions. First, unlike the structural  $\gamma_s(q)$ , the dynamic prediction  $\gamma_d(q)$  is practically independent of the first liquid layer density  $n_s$ . Thus, the collective dynamics of the molecules near the surface furnish a more robust determination of the surface tension, compared with that emerging from its structure. Second, the values of  $\gamma_d(q)$  are quite close to the optimal structural estimation  $\gamma_s(q)$ , which, as stated, corresponds to the value of the surface density  $n_s$  providing the sharpest view of the intrinsic density profile [13]. Results, such as those shown in Figs. 2 and 3, clearly support the ISM definition of the intrinsic surface, providing a consistent link between the structural and dynamical roles of the surface tension; in other words,  $\gamma_s(q) = \gamma_d(q)$ .

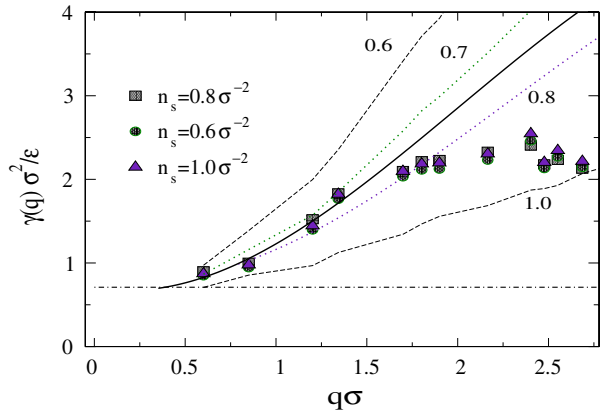


FIG. 3 (color online). The surface tension  $\gamma$  of a Lennard-Jones liquid at  $T = 0.763\epsilon/k$ , density  $\rho = 0.782\sigma^{-3}$ , and  $\eta_0 = 1.85\epsilon\tau/\sigma^3$ . Symbols are obtained from MD simulations, by numerical inversion of the hydrodynamic relation for the decay rate  $\Gamma_d = \Gamma(q, \gamma_d, \eta)$ . Lines corresponds to the ISM structural predictions Eq. (1) for the indicated values of the first layer density  $n_s$ . The optimal  $n_s$  from the structural analysis  $n_s = (0.75 \pm 0.05)\sigma^{-2}$  is shown in solid line (dotted lines indicates the  $0.05\sigma^{-2}$  uncertainty.)

The present dynamical analysis also draws interesting information about the upper wave number  $q_u$  above which surface fluctuations are no longer controlled by surface tension. As shown in Figs. 1 and 2, for  $q > q_u$ , the damping rate  $\Gamma_d$  obtained from  $\langle \xi_q(t) \xi_q(0) \rangle$  gradually deviates from the hydrodynamic trend and saturates to a constant ( $q$ -independent) value,  $\Gamma_u$ . Both  $q_u$  and  $\Gamma_u$  depend on the liquid considered and typically  $q_u \sigma \in [1.5-2.0]$ . What is the origin of such a time scale arising at wavelengths of molecular scale? These very short “waves,” with  $\lambda \lesssim 4\sigma$ , involve very few surface molecules, softly linked together by interatomic forces. Their decorrelation time  $\Gamma_u^{-1}$  should then be of the same order of the diffusion time required for one molecule to move a small (molecular) distance  $\ell$  in the out-of-plane direction. Following this argument,  $\ell \sim \sqrt{D_\perp / \Gamma_u}$ , where  $D_\perp$  is the local coefficient for out-of-plane molecular diffusion, recently calculated in Ref. [21]. Inserting the values of  $D_\perp$  and  $\Gamma_u$  into this estimation, we get  $\ell = (0.19 \pm 0.01)\sigma$  for all the LJ cases considered and  $\ell = (0.18 \pm 0.01)\sigma$  for the SA case. This nice agreement indicates that the surface dynamics at  $q > q_u$  are governed by single molecule diffusion. The crossover from surface tension driven CWs to (Brownian) diffusive motion takes place gradually, as molecular diffusion becomes the slowest “mode” [i.e., for  $\Gamma(q) > D_\perp / \ell^2$ ]. A finer connection with the dynamic structure of the surface can be still made by noting that the “decorrelation length” deduced here  $\ell \simeq 0.2\sigma$ , coincides with the so called “split” displacement  $\Delta x_s$  defined in Ref. [21]. For molecule displacements larger than  $\Delta x_s$ , the mean square displacement in out-of-plane direction ( $\text{MSD}_\perp$ ) starts to deviate from the corresponding in-plane displacements ( $\text{MSD}_\parallel$ ). At larger times,  $\text{MSD}_\perp$  saturates (up to the width of the surface), while  $\text{MSD}_\parallel$  follows a classic diffusion law. In the light of the present findings, the “split” time  $t_s \equiv \Delta x_s^2 / D_\perp$  required for in-plane molecular displacements to become larger than out-of-plane excursions, is also the time needed for an instantaneous molecular configuration to decorrelate to a new one, i.e.,  $\Gamma_u \simeq 1/t_s$ .

To conclude, we have shown that capillary waves in simple liquids are governed by hydrodynamics up to nanometric scales, while molecular diffusion becomes the dominant mode for wavelengths below few particle diameters. In the hydrodynamic regime, the estimation of the surface tension based on its dynamic role  $\gamma_d(d)$  is quite robust with respect to the detailed definition of the intrinsic surface. The optimal surface predicted by the Implicit Sampling Method [13] provides physically consistent structural and dynamical definitions, i.e.,  $\gamma_s(q) = \gamma_d(q)$ . Finally, the monotonic increase of  $\gamma(q)$  disclaims the existence of an enhanced CW regime [9], that would imply a decrease of the surface tension (and damping rate) below the macroscopic prediction.

The robust hydrodynamic behavior found here up to  $T/T_c \approx 0.85$  opens the challenge to extend the ISM to

other interesting scenarios, particularly the critical region of simple liquids, and the surface of viscoelastic or complex fluids, such as polymer-colloid mixtures, with very low surface tension and exotic phenomena, like suppression of thermally excited capillary waves by shear flows [22].

Authors acknowledge fruitful discussions with D. Duque. This work is supported by the Dirección General de Investigación of Spain under the Grant No. FIS2007-65869-C03 and by the Comunidad Autónoma de Madrid under Grant No. s-0505/ESP-0299. R. D-B benefits from the Spanish Ministerio de Educación y Ciencia “Ramon y Cajal” research contract.

---

\*rafael.delgado@uam.es

- [1] U.-S. Jeng *et al.*, *J. Phys. Condens. Matter* **10**, 4955 (1998).
- [2] J. Harden, H. Pleiner, and P. A. Pincus, *J. Chem. Phys.* **94**, 5208 (1991).
- [3] J. Jäckle and K. Kawasaki, *J. Phys. Condens. Matter* **7**, 4351 (1995).
- [4] R. B. Dorshow and L. A. Turkevich, *Phys. Rev. Lett.* **70**, 2439 (1993); H. Kikuchi *et al.*, *Phys. Rev. B* **49**, 3061 (1994).
- [5] A. Madsen *et al.*, *Phys. Rev. Lett.* **92**, 096104 (2004).
- [6] E. Sloutskin *et al.*, *Phys. Rev. E* **77**, 060601(R) (2008).
- [7] K. R. Mecke and S. Dietrich, *Phys. Rev. E* **59**, 6766 (1999).
- [8] P. Tarazona *et al.*, *Phys. Rev. Lett.* **99**, 196101 (2007).
- [9] C. Fradin *et al.*, *Nature (London)* **403**, 871 (2000); S. Mora *et al.*, *Phys. Rev. Lett.* **90**, 216101 (2003).
- [10] P. Pershan, *Colloids Surf. A* **171**, 149 (2000); O. Shpyrko *et al.*, *Phys. Rev. B* **69**, 245423 (2004).
- [11] F. Buff *et al.*, *Phys. Rev. Lett.* **15**, 621 (1965).
- [12] E. Chacón and P. Tarazona, *Phys. Rev. Lett.* **91**, 166103 (2003).
- [13] E. Chacón and P. Tarazona, *J. Phys. Condens. Matter* **17**, S3493 (2005).
- [14] J. Stecki, *J. Chem. Phys.* **109**, 5002 (1998); A. Werner *et al.*, *Phys. Rev. E* **59**, 728 (1999).
- [15] I. M. Mryglod and I. P. Omelyan, *Mol. Phys.* **92**, 913 (1997).
- [16] J. P. Boon and S. Yip, *Molecular Hydrodynamics* (Dover Pubns., New York, 1992).
- [17] G. Ciccotti, G. Jacucci, and I. R. McDonald, *Phys. Rev. A* **13**, 426 (1976).
- [18] We have measured  $\eta(q)$  from the liquid velocity response to a sinusoidal spatial forcing [17]. The best fit to LJ results is  $\eta(q) \simeq \eta_0(1 - 0.079q^2 + 0.011q^3)$ .
- [19] E. Chacon *et al.*, *Phys. Rev. Lett.* **87**, 166101 (2001); E. Velasco *et al.*, *J. Chem. Phys.* **117**, 10777 (2002).
- [20] E. Chacon *et al.*, *Phys. Rev. B* **74**, 224201 (2006); E. Chacon *et al.*, *J. Chem. Phys.* **125**, 014709 (2006).
- [21] D. Duque *et al.*, *J. Chem. Phys.* **128**, 134704 (2008).
- [22] D. Derks *et al.*, *Phys. Rev. Lett.* **97**, 038301 (2006).
- [23] K. Meier *et al.*, *J. Chem. Phys.* **121**, 3671 (2004).